RASĀYAN *J. Chem.*
Vol. 17 | No. 3 |1110-1117| July - September | 2024
ISSN: 0974-1496 | e-ISSN: 0976-0083 | CODEN: RJCABP
http://www.rasayanjournal.com
http://www.rasayanjournal.co.in

SYNTHESIS AND CHARACTERIZATION OF $La_{1-x}Sr_xY_{0.75}Co_{0.25}O_3$ ($0.10 \leq X \leq 0.40$) PEROVSKITE FOR CATHODE MATERIAL OF SOFCs

Sangeeta Devi[1], Naiem Ahmed[1], Neha Sharma[1], Manokamna[2], Aman Sen[3], Shruti Rialach[3] and Surinder Paul[3],✉

[1]Department of Physics, Arni University, Indora, H.P, India
[2]Department of Education, Government of Himachal Pradesh, Shimla H.P, India
[3]Department of Physics and Astronomical Science, CUHP, Dharamshala H.P, India
✉Corresponding Author: surinderpaul79@hpcu.ac.in

ABSTRACT

Solid-oxide fuel cells offer numerous competitive advantages, including higher efficiency and low emissions of greenhouse gases. Material synthesis and selection of its components, including cathode, anode, electrolyte, and interconnect, play a vital role in obtaining the goal. $La_{1-x}Sr_xY_{0.75}Co_{0.25}O_3$ (x= 0.10, 0.20, 0.30, 0.40) perovskite material in the crystalline form of size 185nm to 245nm has been synthesized for its applications. Substituent increases the density value. The material exhibited weight loss on and above 400 ºC temperature confirming the creation of oxygen vacancy on reduction of Y^{3+}/Co^{3+}, and the temperature expansion coefficient decreased with Sr^{2+} substitution. Impedance analysis of all the samples confirmed that the material is dielectric enough and conductivity increased with temperature, frequency, and doping content. The conductivity of the material was found to be more than 100 S/cm above 600 ºC, and the activation energy of the material was found to be 0.19 eV for compositions 0.10 and 0.17 eV for 0.40. Observed parameters confirmed that the material synthesized is appropriate for the cathode component of the cell which can work at an intermediate temperature.

Keywords: Energy, Perovskite, Cathode, Crystalline, Conductivity.

RASĀYAN *J. Chem.*, Vol. 17, No.3, 2024

INTRODUCTION

Solid oxide fuel cells (SOFCs) are fuel cells that have fascinated a lot of interest because of their excellent fuel flexibility, low pollution emissions, high energy transformation efficiency, and electrochemical processes that take place to create electricity.[1-5] Their energy conversion efficiency may reach 65%, which is much greater than that of conventional fuel cells.[6-8] Another distinctive feature of SOFCs is co-generation, which raises the device's efficiency to around 85% by using the heat created during operation to produce electricity. Due to this, SOFCs may also be utilized in steam and gas turbines as combustors. Since the steam transformation is endothermic reaction, a substantial amount of thermal energy is needed to keep it running, and high working temperature of SOFCs provides this energy.[9-11] Expensive catalysts like platinum are rarely necessary when using SOFCs. Nevertheless, SOFCs operating at (~1000}) temperatures have certain drawbacks, including a longer startup time, a shorter cell lifetime because of unfavorable degradation, and reactions between the cell's components, all of which raise the cell's overall cost.[12-14] Titanium based nanoparticles also reported in literature.[15-17] Thus, in order to work around these drawbacks, current research is concentrating on bringing the temperature of operation of SOFCs down by modifying the materials or adding novel materials that could function in the intermediate-temperature ranges at 600–800°C instead of 1000°C or more.[18-21] Higher cathodic polarization at low operative temperatures, it is required to improve cathode materials with suitable material for excellent performance of the cell. But, a fall in the operational temperature drops the cell output by raising the polarization resistance.[22,23] An integral part of a SOFC is the cathode, where oxygen (air) enters in it, and is transformed into ions (O^{2-}). This process is called as ORR that is oxygen reduction reaction. The performance of a device is significantly impacted by the material selection process, which is based on necessity and application. In the same way, material choice is important for SOFC operations. In the last two decades variety of ABO_3 perovskite materials, $La_{0.6}Sr_{0.4}Co_{0.8}Cu_{0.2}O_{3-\delta}$[24], $La_{0.7}Sr_{0.3}Fe_yMn_{1-y}O_3$ (for y

http://doi.org/10.31788/RJC.2024.1738912

equal to 0.10 and 0.40)[25], Nanoscale bismuth oxide impregnated (La,Sr)MnO_3[26], $La_{1.85}Sr_{1.15}Cu_{2-x}Co_xO_{6+\delta}$ intergrowth oxides[27], $La_{1-x}Ca_xFe_{0.75}$ $Co_{0.25}O_3$ {x = 0.05, 0.15, 0.25, 0.35}[28,29],Silver substituted $(La_{0.8}Sr_{0.2})_{1-y}Ag_yMnO_3$ for y equal to 0.05,0.10,0.15 and 0.20 value[30,31] in which Lanthanide and reducible transition metals respectively place at A, and B site with suitable doping of metals like rare and alkaline earth at the Lanthanide site has been reported to synthesized the cathode component of SOFCs.

EXPERIMENTAL

$La_{1-x}Sr_xY_{0.75}Co_{0.25}O_3$ (0.10 ≤x ≤ 0.40) Perovskite cathode material has been synthesized by using yttrium oxide, Lanthanum oxide, Cobalt oxide, and strontium carbonate (99.9% pure) from Sigma Aldrich via the solid-state reaction process. Mixed power in stoichiometric ratio, ball milled for 6 hours. After ball milling, the precursor powder was subjected to 90toC for calcination for twelve hours by conventional way and then ground by a mortal pestle for one hour. 2% polyvinyl alcohol was used as a binder to prepare round pellets of one mm width, ten mm diameter, and as prepared, samples were sintered for four hours at 1250 °C. As prepared, samples were characterized to observe the desired properties.

RESULTS AND DISCUSSION

Structural Properties

The X-ray diffraction (XRD) technique was used to analyze the $La_{1-x}Sr_xY_{0.75}Co_{0.25}O_3$ (0.10 ≤x ≤0.40) material. The prepared material is crystalline in nature, as shown in Fig.-1. ICDD card no. 01-089-5718 was used for peak matching, which showed rhombohedral, R-3c, and 167 crystal structure, space group, and its number, respectively. Peak (400) and (100) specified secondary phases are matched with ICDD card no. 01-073-1334. Variations with a dopant in crystalline size calculated by Shearer's formula, Crystallographic parameters, theoretical density, and experimental density determined by the Archimedes liquid displacement process are displayed in the 01 and 02 table numbers.

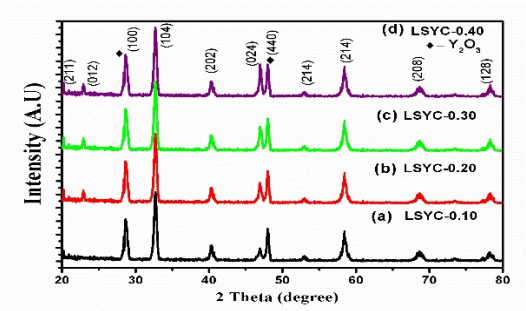

Fig.-1: Pattern of XRD of $La_{1-x}Sr_xY_{0.75}Co_{0.25}O_3$ (0.10 ≤x ≤0.40)

Table-1: Crystallographic Parameters of $La_{1-x}Sr_xY_{0.75}Co_{0.25}O_3$ (0.10 ≤x ≤0.40) Perovskite

Sample	Lattice Parameters (Å)			volume(Å^3)			Crystalline size(nm)
$La_{1-x}Sr_xY_{0.75}Co_{0.25}O_3$	a	b	c	Cell	Occupied	free volume	
x= 0.10	5.47	5.47	13.26	396.75	48.64	0.877	185
x= 0.20	5.46	5.46	13.25	395.01	47.50	0.879	207
x= 0.30	5.46	5.46	13.23	394.40	46.35	0.882	230
x= 0.40	5.45	5.45	13.21	392.37	45.21	0.884	245

Table-2: Density of $La_{1-x}Sr_xY_{0.50}Co_{0.50}O_3$; x equal to (a) for 0.10, (b) for .20, (c) for 0.30, and (d) for 0.40

Sample $La_{1-x}Sr_xY_{0.75}Co_{0.25}O_3$	Density (g cm^{-3})		
	Theoretical (d_{th})	Experimental (d)	(%) (d/d_{th})
x= 0.10	5.41	5.08	93.90
x=0.20	5.43	5.11	94.10
x= 0.30	5.45	5.20	95.41
x= 0.40	5.48	5.28	96.35

Scanning electron microscopy (SEM) used to draw micrographs of the samples. The present work for the two samples with lower composition and higher composition has been given in Fig.-2 (a & b). Size

calculated by Shearer's formula has been verified by the SEM pictures. Defect in ceramics is affected by the neutrality condition of charge increased energy state, and be responsible for cleavage planes in the grains.[32] Also the grains are well-connected with each other, which also confirm the dense nature of the material.

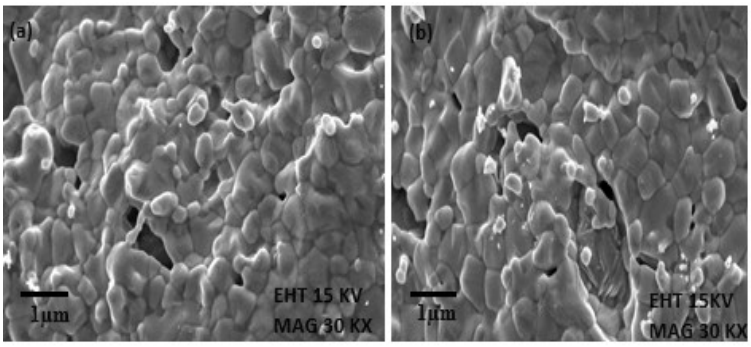

Fig.-2: SEM Pictures of $La_{1-x}Sr_xY_{0.75}Co_{0.25}O_3$ for x equal to (a) 0.10, and (b) 0.40 Samples

Thermal Properties

The component's thermal behavior strongly affects the cell performance, as its stability is one of the significant parameters to reduce the polarization loss during the working of the cell at higher temperatures. Weight Change of the sample for lower doping (0.10) and higher doping (0.40) of as prepared $La_{1-x}Sr_xY_{0.75}Co_{0.25}O_3$ system studied by Thermogravimetric analysis and change in temperature expansion coefficient (TEC) with respect to increasing in dopant respectively has been given in Fig.-3 (a) & (b), and 3 (c) & (d) respectively. The TGA of the samples has been done between 25 °C to 800 °C with a 5 °C heating rate per minute. TGA showed that sharp weight loss results in oxygen vacancy formation, which consequently affects the conductivity. This type of weight loss occurs due to oxidation state change of Co and Y in order to balance the change imbalance, as already reported in the literature.[33-35] A minor TEC alteration was also detected with the substitution of the dopant.

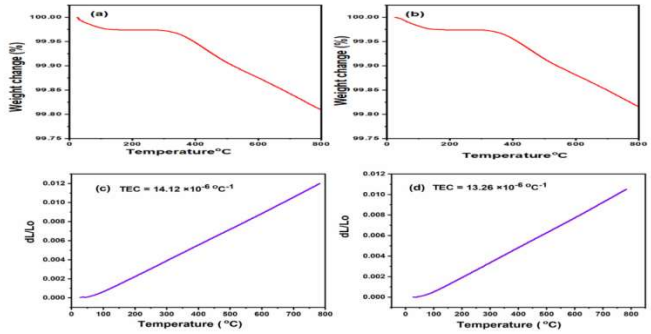

Fig.-3: TGA Curves of $La_{1-x}Sr_xY_{0.75}Co_{0.25}O_3$ for x Equal to (a) 0.10, and (b) 0.40 Samples and TEC of $La_{1-x}Sr_xY_{0.75}Co_{0.25}O_3$ for x Equal to (a) 0.10, and (b) 0.40

Impedance Spectroscopy

Dielectric constant ε′ (real part) vs. frequency of $La_{1-x}Sr_xY_{0.75}Co_{0.25}O_3$ for (x = 0.10, 0.20, 0.30, 0.40) is described in figure 4 (a, b, c and d), and dielectric constant ε″ (imaginary part) vs. frequency of $La_{1-x}Sr_xY_{0.75}Co_{0.25}O_3$ for (x = 0.10, 0.20, 0.30, 0.40) is shown in Fig.-5 (a, b, c and d). In some cases, ε′ and ε″ sharp falls were observed at lower frequencies, whereas linear behavior occurred at higher frequencies. This type of behavior was well explained and earlier reported by the dipolar relaxation phenomenon.[36] Negligible dielectric loss is observed because of the absence of a peak in the imaginary part; consequently, polarizations are totally dominated by the hopping mechanism. All types of polarization electronic, space charge, ionic, and dipolar contribution occur at low-frequency regions while both ε′ and ε″ delay the switching signal of orientation especially dipolar, resulting in lined variation as numerous polarizations are sieved out among the overall polarizability, and then shrink polarization in that region.[37-40] Also, it is markedly specified that ε′ as well as ε″ rises with Sr content which may without dipolar polarization however arise as a consequence of the contribution of interfacial polarization.

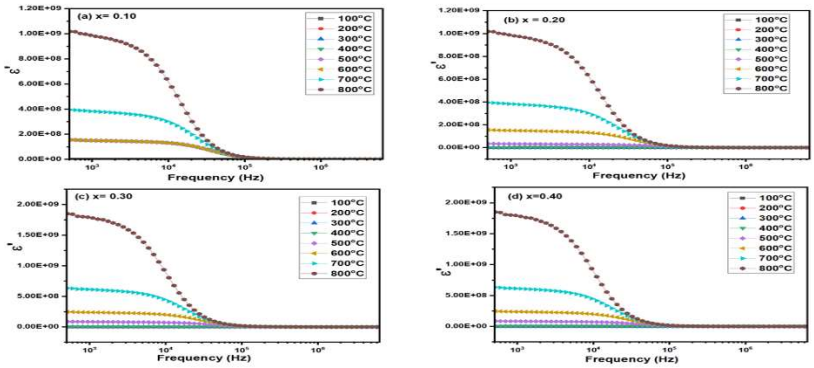

Fig.-4: Dielectric Constant ε′ (real part) vs Frequency of $La_{1-x}Sr_xY_{0.75}Co_{0.25}O_3$ for the Composition (x= 0.10, 0.20, 0.30, 0.40) Perovskite

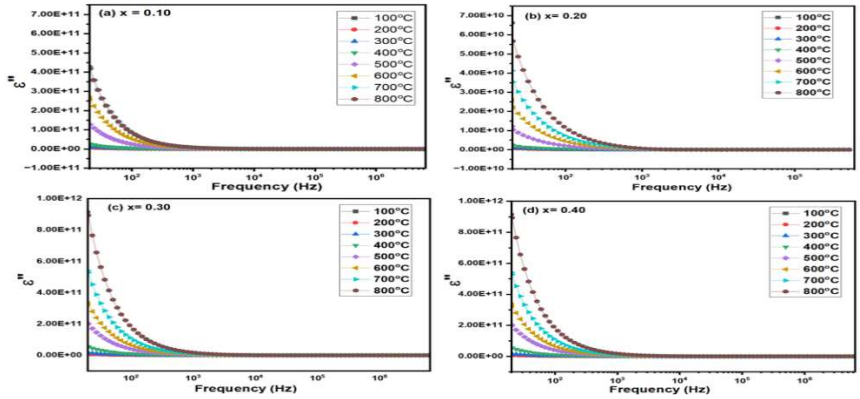

Fig.-5: Dielectric Constant ε′ (imaginary part) vs Frequency of $La_{1-x}Sr_xY_{0.75}Co_{0.25}O_3$ for the Composition (x= 0.10, 0.20, 0.30, 0.40)

In impedance, real part (Z′) changes with frequency of $La_{1-x}Sr_xY_{0.75}Co_{0.25}O_3$ for (0.10 ≤x ≤0.40) described in figure 6(a, b, c &d) and imaginary part (Z″) changes with frequency of $La_{1-x}Sr_xY_{0.75}Co_{0.25}O_3$ for (0.10 ≤x ≤0.40) shown in Fig.-7(a, b, c &d). It is obviously found that the magnitude of Z′ at low temperatures is greater, and observed that falls with frequency, subsequently showing a characteristic negative temperature coefficient of resistance; approving that electrical conductivity upsurges. At high frequency, the merging of Z′ and Z″ specify the fall of barrier properties and disappearance of space charge polarization respectively.[41-43]

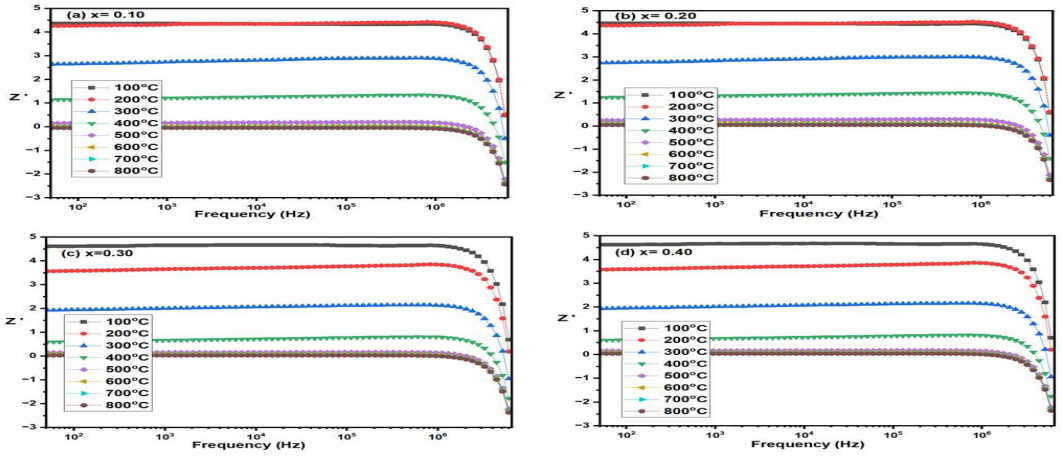

Fig.-6: Z′ (Real Impedance Part) vs Frequency of $La_{1-x}Sr_xY_{0.75}Co_{0.25}O_3$ for the Composition (x= 0.10, 0.20, 0.30, 0.40)

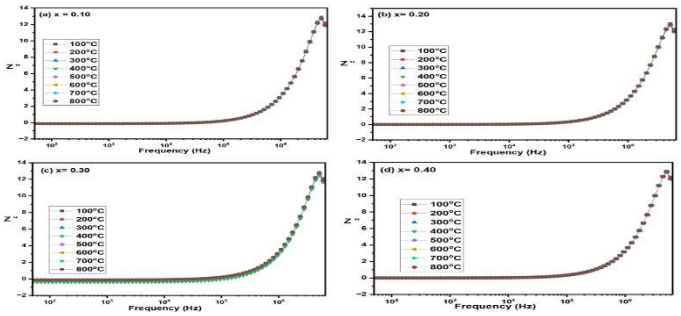

Fig.-7: Z″ (Imaginary Impedance Part) vs Frequency of $La_{1-x}Sr_xY_{0.75}Co_{0.25}O_3$ for (x= 0.10, 0.20, 0.30, 0.40) Perovskite

Electrical Properties

Universal power law missioned in the following line used to obtain conductivity:

$$\sigma_{ac} = (\omega\, \varepsilon_0) \times \varepsilon'(\omega) \times \mathrm{Tan}\delta \qquad (1)$$

Where ω represents angular frequency, ε_0 represents free space permittivity, and Tan δ represents loss in the dielectric. Variation of the conductivity vs. temperature has been show in Fig.-8(a) for $La_{1-x}Sr_xY_{0.75}Co_{0.25}O_3$ (x= 0.10, 0.20, 0.30, 0.40) perovskite and Arrhenius curves plotted to calculate the activation energy of the material shown in Fig.-8(b). The obtained value of conductivity for intermediate temperatures of 600 ^{0}C and 800 ^{0}C has been given in Table number 4. It has been observed that strontium doping increased the conductivity and consequently activation energy decreased. This type of perovskite material already has been reported in the literature.[44-46] Energy of activation in addition to conductivity of the $La_{1-x}Sr_xY_{0.75}Co_{0.25}O_3$ for ($0.10 \leq x \leq 0.40$) perovskite has been given in Table-3.

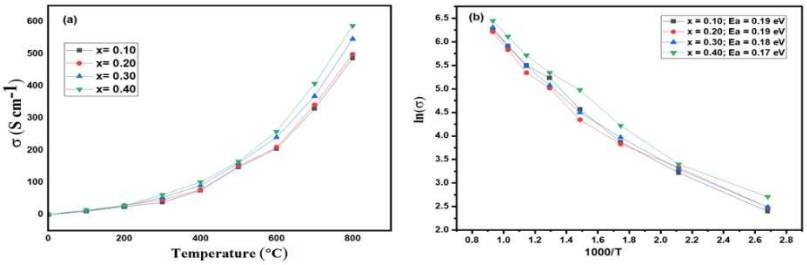

Fig.-8: σ (Conductivity) and E_a (Activation Energy) vs Temperature of $La_{1-x}Sr_xY_{0.75}Co_{0.25}O_3$ for the Composition (x= 0.10, 0.20, 0.30, 0.40)

Table-3: σ (Conductivity) and E_a (Activation Energy) of the $La_{1-x}Sr_xY_{0.75}Co_{0.25}O_3$ for the Composition (x= 0.10, 0.20, 0.30, 0.40)

Samples	Conductivity (Scm^{-1})		Ea (eV)
$La_{1-x}Sr_xY_{0.75}Co_{0.25}O_3$	600 ^{0}C	800 ^{0}C	
x = 0.10	210	490	0.19
x = 0.20	215	515	0.19
x = 0.30	222	555	0.18
x = 0.40	230	580	0.17

CONCLUSION

$La_{1-x}Sr_xY_{0.75}Co_{0.25}O_3$ for ($0.10 \leq x \leq 0.40$) ceramics type perovskite material has been synthesized. Precursor powder which heated at 900°C for twelve hours, and sintered for four hours at 1250 °C. Crystalline size 185nm to 245nm has been confirmed by x-ray diffraction of the as-prepared samples. Substituent increases the density of the material. Grains are well connected with each other, which also confirms the dense nature of the material. The density of the material has been found to increase with strontium metal doping. The material showed weight loss at temperatures above 400 °C,^{0} as confirmed by TGA. Temperature expansion coefficient (TEC) was found to be 14.12×10^{-6} $^0C^{-1}$ for x = 0.10 and 13.26

$\times 10^{-6}\ ^{0}C^{-1}$ for x = 0.40. At low frequencies, the dielectric constant is high, and shows linear behavior, with negligible polarization. Conductivity of the material was found to be greater than 100 S/cm on and above 600 °C, and also activation energy be 0.19 eV and 0.17 eV has been found for compositions 0.10 and 0.40, respectively. Observed parameters confirmed that the material synthesized can be suitable for the cathode component of an intermediate-temperature solid oxide fuel cell.

ACKNOWLEDGMENTS

The authors would like to thank the authorities of their institutions for providing needful cooperation and support.

CONFLICT OF INTERESTS

The authors have no conflict of interest.

AUTHOR CONTRIBUTIONS

All the authors contributed significantly to this manuscript, participated in reviewing/editing, and approved the final draft for publication. The research profile of the authors can be verified from their ORCID IDs, given below:

Sangeeta Devi https://orcid.org/0000-0002-7397-1655
Naiem Ahmed https://orcid.org/0000-0001-7423-0368
Neha Sharma https://orcid.org/0000-0002-2487-2458
Manokamna https://orcid.org/0000-0002-5389-7953
Aman Sen https://orcid.org/0009-0003-3765-3099
Shruti Rialach https://orcid.org/0009-0006-0292-4807
Surinder Paul https://orcid.org/0000-0003-4377-6880

REFERENCES

1. S. Singhal, *Solid State Ionic,* **135,** 305(2000), https://doi.org/10.1016/S0167-2738(00)00452-5
2. E. Bucher, *Berg Huettenmaenn Monatsh*, **156,** 423(2011), https://doi.org/10.1007/s00501-011-0030-3
3. N. Ahmed, S. Devi, M.A. Dar, S.K.M. Ibrahim, A. Sharma, N. Sharma, S. Paul, S.R. Ahamed, *Indian Journal of Physics*, **98,** 877(2024), https://doi.org/10.1007/s12648-023-02860-3
4. J. Larminie, A. Dicks, 1st ed., Wiley, (2003), https://doi.org/10.1002/9781118878330
5. S. Paul, B. Bharti, R. Kumar, P. Sharma, G.K. Bhargava, *Springer Nature* Singapore, Singapore,113(2023), https://doi.org/10.1007/978-981-99-2583-4_7
6. A.B. Stambouli, E. Traversa, *Renewable and Sustainable Energy Reviews,* **6,** 433(2002), https://doi.org/10.1016/S1364-0321(02)00014-X
7. M.P. Binitha, P.P. Pradyumnan, *MaterialsToday: Proceedings,* S2214785323016413(2023), https://doi.org/10.1016/j.matpr.2023.03.574
8. O. Yamamoto, *Electrochimica Acta,* **45,** 2423(2000), https://doi.org/10.1016/S0013-4686(00)00330-3
9. R.M. Ormerod, *Chemical Society Reviews,* **32,** 17 (2003), https://doi.org/10.1039/b105764m
10. S. Mekhilef, R. Saidur, A. Safari, *Renewable and Sustainable Energy Reviews*, **16,** 981(2012), https://doi.org/10.1016/j.rser.2011.09.020
11. Manokamna, S. Paul, A. Kumar, D.K. Sharma, K.L. Singh, G. Bhargava, A.P. Singh, in: Indore, India, p. 020136(2021), https://doi.org/10.1063/5.0061372
12. L. Zhang, Y. Xing, H. Xu, H. Wang, J. Zhong, J. Xuan, C *Energy Conversion and Management*, **139,** 79(2017), https://doi.org/10.1016/j.enconman.2017.02.045
13. Manokamna, S. Paul, A. Kumar, A. Singh, K.L. Singh, G. Bhargav, A.P. Singh, *Materials Today: Proceedings*, **45,** 4639 (2021), https://doi.org/10.1016/j.matpr.2021.01.095
14. J. Lewis, *International Journal of Hydrogen Energy*, **39,** 21896(2014), https://doi.org/10.1016/j.ijhydene.2014.05.177

15. Ankansha, N. Ahmed, Manokamna, A. Singh, S. Paul, *Materials Today: Proceedings,* **62**, 6385(2022), https://doi.org/10.1016/j.matpr.2022.03.384
16. N.Ahmed, S. Devi, Ankansha, Manokamna, A. Singh, S. Paul, *Materials Today: Proceedings,* **60,** 2188(2022), https://doi.org/10.1016/j.matpr.2022.02.440
17. N. Ahmed, A. Manokamna, N. Singh, N. Sharma, S. Paul, *Materials Today: Proceedings,* **65,** 3288(2022), https://doi.org/10.1016/j.matpr.2022.05.390
18. L. Ma, J. Gong, C. Jin, D. Yang, J. Hou, *Journal of Alloys and Compound,* **945,** 169359(2023), https://doi.org/10.1016/j.jallcom.2023.169359
19. S. Paul, V. Anand, Noorjahan, V. Duggal, Manokamna, *Materials Today: Proceedings*, S2214785323046916(2023), https://doi.org/10.1016/j.matpr.2023.09.029
20. C. Ouyang, M. Zoghi, H. Habibi, *International Journal of Hydrogen Energy*, **60,** 1101(2024), https://doi.org/10.1016/j.ijhydene.2024.02.243
21. W. Zhang, X. Kuang, W. Zhang, D. Yan, L. Jia, *International Journal of Hydrogen Energy*, **62**, 1171(2024), https://doi.org/10.1016/j.ijhydene.2024.02.329
22. A. Jun, J. Kim, J. Shin, G. Kim, *ChemElectroChem,* **3,** 511(2016), https://doi.org/10.1002/celc.201500382
23. A. Tesfai, J.T.S. Irvine, *Comprehensive Renewable Energy*, Elsevier, pp.274–289(2012), https://doi.org/10.1016/B978-0-12-819727-1.00195-3
24. B. Lin, J. Chen, Y. Ling, X. Zhang, Y. Jiang, L. Zhao, X. Liu, G. Meng, *Journal of Power Sources*, **195,** 1624(2010), https://doi.org/10.1016/j.jpowsour.2009.09.039
25. S. Paul, Manokamna, A. Kumar, S. Kaur, A. Singh, A. Kumar, *Materials Today: Proceeding,* **56,** 1684 (2022), https://doi.org/10.1016/j.matpr.2021.10.319
26. Z. Jiang, L. Zhang, K. Feng, C. Xia, *Journal of Power Sources*, **185,** 40(2008), https://doi.org/10.1016/j.jpowsour.2008.07.003
27. Y.N. Kim, A. Manthiram, *Electrochimica Acta,* **70,** 375(2012), https://doi.org/10.1016/j.electacta.2012.03.087
28. S. Devi, Manokamna, R. Kumar, S. Paul, *Materials Today: Proceedings*, S2214785322075034(2023), https://doi.org/10.1016/j.matpr.2022.12.132
29. S. Devi, N. Ahmed, Manokamna, A. Singh, S. Paul, *Materials Today: Proceedings*, **60,** 1989(2022), https://doi.org/10.1016/j.matpr.2022.01.214
30. S. Paul, *Materials Today: Proceedings*, S2214785323009835(2023), https://doi.org/10.1016/j.matpr.2023.02.418
31. S. Paul, Manokamna, V. Duggal, V.S. Jaswal, R. Kumar, *Materials Today: Proceeding,* S2214785323003929(2023), https://doi.org/10.1016/j.matpr.2023.01.302
32. M.D. Antonik, R.J. Lad, **10**, 669(1992), https://doi.org/10.1116/1.577707
33. A. Weber, E. Ivers-Tiffée, *Journal of Power Sources*, **127**, 273(2004), https://doi.org/10.1016/j.jpowsour.2003.09.024
34. L. Ma, J. Gong, C. Jin, D. Yang, J. Hou, *Journal of Alloys and Compounds,* **945,** 169359(2023), https://doi.org/10.1016/j.jallcom.2023.169359
35. J. Richter, P. Holtappels, T. Graule, L. Gauckler, *Solid State Ionics*, **179,** 2284(2008), https://doi.org/10.1016/j.ssi.2008.08.007
36. M. Kumar, K.L. Yadav, *Journal of Applied Physics*, **100,** 074111(2006), https://doi.org/10.1063/1.2349491
37. E. Bouzaiene, Ch. Rayssi, J. Dhahri, Ab. Afef, H. Belmabrouk, M.A. Albedah, *Journal of Material Science: Materials in Electronics*, **34**, 285(2023), https://doi.org/10.1007/s10854-022-09673-w
38. S. Paul, Manokamna, A. Kumar, D.K. Sharma, A. Singh, A. Kumar, *Rasayan Journal of Chemistry*, **15(1),** 210(2022), https://doi.org/10.31788/RJC.2022.1516751
39. M. Coşkun, Ö. Polat, F.M. Coşkun, Z. Durmuş, M. Çağlar, A. Türüt, *RSC Adv*ances, **8,** 4634(2018), https://doi.org/10.1039/C7RA13261A
40. O. Polat, M. Coskun, Y. Yildirim, P. Roupcova, D. Sobola, C. Sen, Z. Durmus, M Caglar, A. Turut, *Journal of Alloys and Compounds*, **963**, 170939(2023), https://doi.org/10.1016/j.jallcom.2023.170939

41. U. Dash, S. Sahoo, P. Chaudhuri, S.K.S. Parashar, K. Parashar, *Journal of Advanced Ceramics*, **3**, 89 (2014), https://doi.org/10.1007/s40145-014-0094-0
42. B. Tiwari, T. Babu, R.N.P. Choudhary, *Physica Scripta*, **95**(2020), https://doi.org/10.1088/14024896/abbc9e
43. B. Tiwari, R.N.P. Choudhary, *Journal of Alloys and Compound,* **493,** 1(2010), https://doi.org/10.1016/j.jallcom.2009.11.120
44. S. Song, J. Liu, H. Wang, Y. Wang, X. Huang, M. Zeng, *Journal of Alloys and Compound,* **966**, 171602(2023), https://doi.org/10.1016/j.jallcom.2023.171602
45. Manokamna, S. Paul, A. Singh, K. L. Singh, G. Bhargava, A. P. Singh, R*asayan Journal of Chemistry*, **14(2)**, 1019(2021), http://dx.doi.org/10.31788/RJC.2021.1426153
46. I. Kosacki, *Solid State Ionics,* **152**, 431(2002), https://doi.org/10.1016/S0167-2738(02)00382-X

[RJC-8912/2024]